

# Dalton Transactions

Accepted Manuscript



This is an *Accepted Manuscript*, which has been through the Royal Society of Chemistry peer review process and has been accepted for publication.

*Accepted Manuscripts* are published online shortly after acceptance, before technical editing, formatting and proof reading. Using this free service, authors can make their results available to the community, in citable form, before we publish the edited article. We will replace this *Accepted Manuscript* with the edited and formatted *Advance Article* as soon as it is available.

You can find more information about *Accepted Manuscripts* in the [Information for Authors](#).

Please note that technical editing may introduce minor changes to the text and/or graphics, which may alter content. The journal's standard [Terms & Conditions](#) and the [Ethical guidelines](#) still apply. In no event shall the Royal Society of Chemistry be held responsible for any errors or omissions in this *Accepted Manuscript* or any consequences arising from the use of any information it contains.

**Application of hydrophobically modified water-soluble polymers  
for the dispersion of hydrophobic magnetic nanoparticles  
in aqueous media**

Zacharoula Iatridi<sup>1</sup>, Violetta Georgiadou<sup>2</sup>, Melita Menelaou<sup>2</sup>, Catherine Dendrinou-Samara<sup>2\*</sup> and Georgios Bokias<sup>1\*</sup>

<sup>1</sup>. *Department of Chemistry, University of Patras, GR-26504 Patras, Greece*

<sup>2</sup>. *Department of Chemistry, Aristotle University of Thessaloniki, GR-54124  
Thessaloniki, Greece*

\*Corresponding Authors

C. Dendrinou-Samara, Phone (+30) 2310-997876; Fax (+30) 2310-997876; E-mail  
[samkat@chem.auth.gr](mailto:samkat@chem.auth.gr)

G. Bokias, Phone (+30) 2610-997102; Fax (+30) 2610-997122; E-mail [bokias@upatras.gr](mailto:bokias@upatras.gr)

## Abstract

Hydrophobically modified water-soluble polymers (HMWSP), comprised by a poly(sodium methacrylate) (PMANa) or poly(sodium acrylate) (PANa) backbone and pendent dodecyl methacrylate (DMA) or dodecyl acrylamide (DAAm) chains, respectively, were synthesized. The hydrophobic content of the copolymers, P(MANa-co-DMA) and P(ANa-co-DAAm), is in the range of 0 to 25 mol%, while their weight-average molar mass varies from  $\sim 10000$  up to  $\sim 75000$ . Their self-assembly behavior in dilute aqueous solutions was followed through Nile Red probing, DLS and TEM measurements. The critical micellization concentration (CMC) is mainly controlled by the hydrophobic content and not the molar mass of the copolymers. Above CMC, spherical and spherical large-compound micelles are identified by DLS and TEM. Moreover, oleylamine coated  $\text{CoFe}_2\text{O}_4$  nanoparticles ( $\text{CoFe}_2\text{O}_4@OAm$  MNPs) of 9.4 nm with saturation magnetization  $M_s=85$  emu/g were solvothermally prepared. The hydrophobic  $\text{CoFe}_2\text{O}_4@OAm$  MNPs were successfully encapsulated into the hydrophobic cores of the structures formed by the copolymers above CMC through a solvent mixing procedure, and in that way hydrophilic  $\text{CoFe}_2\text{O}_4@HMWSP$  nanohybrids were resulted. For comparison reasons, two alternate phase transfer approaches were also used to convert  $\text{CoFe}_2\text{O}_4@OAm$  MNPs to hydrophilic; a) addition of a coating layer by cetyltrimethyl ammonium bromide (CTAB) and b) by ligand exchange procedure with 2,3-dimercaptosuccinic acid (DMSA). NMR transverse relaxivity measurements of the aqueous suspensions of  $\text{CoFe}_2\text{O}_4@P(ANa-co-DAAm)$ ,  $\text{CoFe}_2\text{O}_4@CTAB$  and  $\text{CoFe}_2\text{O}_4@DMSA$  were recorded and  $r_2$  relaxivity was determined.  $\text{CoFe}_2\text{O}_4@CTAB$  demonstrated the highest  $r_2$  relaxivity  $554.0 \text{ mM}^{-1}\text{s}^{-1}$ , while  $\text{CoFe}_2\text{O}_4@P(ANa-co-DAAm)$  and

CoFe<sub>2</sub>O<sub>4</sub>@DMSA showed lower values at 313.6 mM<sup>-1</sup>s<sup>-1</sup> and 76.3 mM<sup>-1</sup>s<sup>-1</sup>, respectively.

## Introduction

The self-assembly behavior of amphiphilic copolymers in aqueous media has been a very attractive topic for decades as they find use in numerous applications like drug delivery systems, cosmetics, paints, colloids, emulsifiers, coatings and rheology modifiers.<sup>1</sup> The leading forces for self-association of amphiphilic polymer chains are hydrophobic interactions along with intramolecular electrostatic interactions. In the case of amphiphilic polyelectrolytes, hydrophobic monomer units and hydrophilic electrolyte monomer units are attached on the same polymer chain. While amphiphilic block copolymers have been extensively investigated,<sup>1b-d,2</sup> the self-assembly of random amphiphilic copolymers is becoming more and more intriguing. Numerous scientific groups have reported a variety of morphologies<sup>3</sup> of random amphiphilic copolymer self-assemblies, like spherical micelles, flower-like micelles, large-compound or multicore micelles, vesicles, etc.

Random amphiphilic copolymers can be either linear, consisted of small hydrophilic and hydrophobic units, or of a comb-like structure, consisted of a hydrophilic backbone (for example, poly(sodium acrylate),<sup>4</sup> polyacrylamide<sup>5</sup> or natural derivatives<sup>6</sup>) and long alkyl hydrophobic pendent chains (typically, dodecyl- or octadecyl- chains). This last class is usually called hydrophobically modified water-soluble polymers (HMWSP)<sup>7</sup> and has been extensively studied and proposed for applications as rheology modifiers, emulsion stabilizers, etc.<sup>8</sup>

Cobalt ferrite nanoparticles (CoFe<sub>2</sub>O<sub>4</sub> MNPs) are among the magnetic nanoparticles that have been proposed for several bioapplications<sup>9</sup> such as contrast enhancement candidates in magnetic resonance imaging (MRI), hyperthermia agents,

magnetically tagging devices of bioentities and drug carriers.<sup>10</sup> Although wet chemistry preparation methods in organic solvents are highly efficient in controlling the main features of magnetic nanoparticles like the size, shape, crystallinity and monodispersity, the hydrophobic nature of the derived MNPs impediments their direct use in bioapplications and further functionalization is needed.<sup>11</sup>

Since hydrophilicity is essential for *in vitro* and *in vivo* applications, phase transfer becomes necessary. In general, several strategies exist and applied for phase transfer:<sup>12</sup> a) ligand exchange where a hydrophobic ligand is replaced by a hydrophilic one, b) ligand modification with a variety of bioactive molecules, c) additional coating layers through hydrophobic interactions with the original ligand, d) silanization and e) polymer coating, where hydrophobic MNPs are encapsulated in the hydrophobic domains of the supramolecular structures formed by amphiphilic molecules through hydrophobic interactions and Van der Waals forces. The concept of using amphiphilic block copolymers for the stabilization of hydrophobic MNPs in water has been widely exploited.<sup>13</sup> In contrast, literature on the use of HMWSP to stabilize hydrophobic MNPs in aqueous media is relatively poor.<sup>14</sup> Nevertheless, such applications of HMWSP are of particular interest, since it is much easier to be synthesized than block copolymers, using a one-step synthetic procedure (free radical polymerization of adequate monomers or chemical modification of the backbone).

In the present study, the possibility of using the micelle-like structures formed by HMWSP to stabilize hydrophobic  $\text{CoFe}_2\text{O}_4@OAm$  MNPs in aqueous media was evaluated. Thus, a series of HMWSP consisted of a poly(sodium methacrylate) backbone (PMANa) and dodecyl- pendent chains were prepared through free radical copolymerization of methacrylic acid (MAA) and dodecylmethacrylate (DMA). The synthetic conditions were adjusted, in order to vary the dodecyl-content and the

molecular weight of the samples. Moreover, a sample of a comparable hydrophobic content was prepared through grafting of dodecyl chains onto a poly(sodium acrylate) backbone (PANa), in an attempt to investigate the possible influence of the synthetic protocol (copolymerization or “grafting-to” methodology). The synthesis and characterization of the HMWSP used and the hydrophobically modified  $\text{CoFe}_2\text{O}_4@\text{OAm}$  MNPs is first discussed in the present work. The major part of the work is devoted to the investigation of the ability of these HMWSP to disperse the hydrophobically modified  $\text{CoFe}_2\text{O}_4@\text{OAm}$  MNPs in water ( $\text{CoFe}_2\text{O}_4@\text{HMWSP}$ ), in conjunction with the self-organization properties of the polymers in aqueous environment. Moreover, NMR relaxivity ( $r_2$ ) studies of aqueous suspensions of  $\text{CoFe}_2\text{O}_4@\text{HMWSP}$  was performed and compared with the hydrophilic modified  $\text{CoFe}_2\text{O}_4@\text{OAm}$  MNPs, resulted by i) an additional coating layer with the positively charged molecule cetyltrimethyl ammonium bromide, ( $\text{CoFe}_2\text{O}_4@\text{CTAB}$ ) and ii) ligand exchange through 2,3-dimercaptosuccinic acid ( $\text{CoFe}_2\text{O}_4@\text{DMSA}$ ).

## Experimental Part

### Materials

The monomer methacrylic acid (MAA), the fluorescent probe Nile Red, dodecylamine (DAm) as well as iron(III) acetylacetonate ( $\geq 97.0\%$ ,  $\text{Fe}(\text{acac})_3$ ) were purchased from Fluka, while the monomer dodecyl methacrylate (DMA) was obtained from Acros. The homopolymer poly(acrylic acid) (PAA) with a molecular weight of 5000 g/mol, the initiator azobisisobutyronitrile (AIBN), the coupling agent  $N,N'$ -dicyclohexylcarbodiimide (DCC), cobalt(III) acetylacetonate ( $\geq 99.9\%$ ,  $\text{Co}(\text{acac})_3$ ), oleylamine (OAm) and the solvents  $N,N$ -dimethylformamide (DMF), tetrahydrofuran (THF), dimethyl sulfoxide (DMSO), chloroform, ethanol, methanol, petroleum ether, deuterated dimethyl sulfoxide ( $d_6$ -DMSO) and deuterated water

(D<sub>2</sub>O) were all purchased from Aldrich. Meso-2,3-Dimercaptosuccinic acid (DMSA) was purchased from Tokyo Chemical Industry (TCI) Co. Ltd. and cetyltrimethyl ammonium bromide (CTAB) (98.0%) was purchased from Alfa Aesar. Ultrapure 3D-water was obtained by means of a SG Waters apparatus.

### **Synthesis of amphiphilic copolymers and CoFe<sub>2</sub>O<sub>4</sub>@OAm nanoparticles**

Synthesis of the P(MANa-co-DMA) copolymers. Typically, a THF solution of MAA, DMA and AIBN was added in a round-bottom flask equipped with a reflux condenser. The mixture was degassed with Ar for 2 hours and the reaction was performed by heating at 70 °C and left overnight under stirring. The polymers were recovered through precipitation in petroleum ether and dried under vacuum at 40 °C. The acid form of the copolymer, P(MAA-co-DMA), was transformed to the sodium salt form, P(MANa-co-DMA), through dissolution in an aqueous NaOH solution. The copolymer was purified through dialysis and recovered through freeze-drying.

Synthesis of the P(ANa-co-DAAm) copolymer. Briefly, in a three-necked flask equipped with a reflux condenser proper amounts of PAA (M<sub>w</sub> = 5000 g/mol) and DAm were firstly dissolved in DMF at 60 °C. Then, DCC dissolved in a small amount of DMF was added dropwise to the solution and the mixture was left under stirring at 60 °C. After 24h, the solution was cooled at room temperature; vacuum filtered to remove the unwanted dicyclohexyl urea byproduct and the necessary volume of a 1M NaOH aqueous solution was added in the copolymer solution. The sodium salt form of the precipitated copolymer was washed several times with DMF and then with methanol in order to remove unreacted segments and byproducts. The final polymer was filtered under vacuum and dried in a vacuum oven at 60 °C.

Solvothermal synthesis of CoFe<sub>2</sub>O<sub>4</sub>@OAm nanoparticles. Based on our previous results<sup>15</sup> CoFe<sub>2</sub>O<sub>4</sub>@OAm MNPs have been prepared solvothermally by dissolving 1.8 mmol of Fe(acac)<sub>3</sub> and 0.9 mmol Co(acac)<sub>3</sub> in 12 mL of OAm. The resulting solution was stirred thoroughly and then transferred into a 23 mL Teflon-lined stainless-steel autoclave. The autoclave was placed in an electrical oven and temperature was raised up to 200 °C (4 °C/min) for 24 h. Then the autoclave was cooled to room temperature with a steady rate of 5 °C/min and the product was washed with ethanol. The washing process via centrifugation cycles (10000 rpm) was repeated at least three times, and the excess of OAm and unreacted precursors was removed by discarding the supernatant. Finally, CoFe<sub>2</sub>O<sub>4</sub>@OAm MNPs were obtained as a black-brown precipitate.

#### **Stabilization of hydrophobic CoFe<sub>2</sub>O<sub>4</sub>@OAm MNPs in water**

Preparation of aqueous CoFe<sub>2</sub>O<sub>4</sub>@HMWSP dispersions. The hybrid CoFe<sub>2</sub>O<sub>4</sub>@HMWSP materials were prepared using a solvent mixing methodology. Briefly, a proper amount of HMWSP was dissolved in 3D water and left under stirring overnight. A small volume of a THF dispersion of CoFe<sub>2</sub>O<sub>4</sub>@OAm MNPs was added in the aqueous polymer solution. The polymer/MNPs mixing ratio was adjusted to 10/1 by weight) and sonicated in a Branson 1510 70W, 40 kHz sonicator. No precipitation was observed upon mixing the polymer solution with the CoFe<sub>2</sub>O<sub>4</sub>@OAm dispersion. The mixture was left at 40 °C until full evaporation of THF. At this stage, precipitation of a fraction of MNPs was eventually observed. This fraction was discarded and the supernatant was used for further studies.

Preparation of aqueous CoFe<sub>2</sub>O<sub>4</sub>@CTAB dispersions. The as-prepared hydrophobic CoFe<sub>2</sub>O<sub>4</sub>@OAm MNPs were converted to hydrophilic via the cationic surfactant CTAB (CoFe<sub>2</sub>O<sub>4</sub>@CTAB) following a previously reported method.<sup>16</sup> An aqueous



solution of CTAB (0.02 M) and a suspension of  $\text{CoFe}_2\text{O}_4@\text{OAm}$  MNPs (3 mg) in chloroform (0.5 mL) were prepared and mixed to lead to an oil-in-water microemulsion. The resulted mixture was sonicated for more than 5 h until the chloroform was completely evaporated, leaving a brownish aqueous solution abbreviated as  $\text{CoFe}_2\text{O}_4@\text{CTAB}$  MNPs.

Preparation of aqueous  $\text{CoFe}_2\text{O}_4@\text{DMSA}$  dispersions. A ligand exchange method was followed where the hydrophobic surface of  $\text{CoFe}_2\text{O}_4$  MNPs was modified to hydrophilic. A mixture of the capping agent DMSA (10 mg) in DMSO (0.5 mL) was added into a mixture of  $\text{CoFe}_2\text{O}_4@\text{OAm}$  MNPs (10 mg) in toluene (3 mL).<sup>17</sup> The resulted mixture was sonicated for 15 min and stirred for 24 h at room temperature. The supernatant was discarded and the resulted  $\text{CoFe}_2\text{O}_4@\text{DMSA}$  MNPs were successfully mixed and centrifuged with ethanol several times to remove free OAm molecules before dispersed in water. The pH of the aqueous suspension increased up to 10 with 1 M NaOH solution in order to deprotonate the carboxylic groups and thiol groups (pK 9.2) of the DMSA<sup>17</sup> and then adjusted to 5 with 1 M  $\text{HNO}_3$  solution in order to achieve better dispersion of the  $\text{CoFe}_2\text{O}_4@\text{OAm}$  MNPs.<sup>17,18</sup> The resulting suspension is stable in water for a prolonged period of time and named as  $\text{CoFe}_2\text{O}_4@\text{DMSA}$  MNPs.

### Characterization Techniques

<sup>1</sup>H-NMR spectra of the copolymers in  $d_6$ -DMSO or  $\text{D}_2\text{O}$  were obtained on a Bruker Advance DPX 400 MHz spectrometer. The acid form of the copolymers, soluble in THF, was used for the Gel Permeation Chromatography (GPC) characterization. Two PLgel MiniMix columns “C” and “D” (molecular range 4000-340000 g/mol) were used and calibrated with polystyrene standards. THF was used as eluent. The elution rate was 0.5 mL/min. Powder X-ray diffraction (XRD) diagram was obtained by

using a 2-cycle Rigaku Ultima + diffractometer (40 kV, 30 mA, CuK $\alpha$  radiation) with Bragg-Brentano geometry (detection limit 2% approximately). Size was estimated by taking the full width at half-maximum (FWHM) of the most intense peak (311) and based on the Debye-Scherrer equation.<sup>19</sup> Magnetic measurements were performed in a 1.2H/CF/ HT Oxford Instruments VSM at 300K as function of the applied field (1 T) and a Superconducting Quantum Interference Device (Quantum Design MPMS-5 SQUID). Elemental analysis was tested by inductively coupled plasma optical emission spectroscopy (ICP-OES, ICP Simultané VARIAN Vista Axial)

### **Physicochemical characterization**

Nile Red fluorescence probing. Steady-state fluorescence spectra of Nile Red were recorded on a Perkin Elmer LS50B luminescence spectrometer. A small volume (5  $\mu$ L) of a stock THF solution, containing  $1 \times 10^{-3}$  M Nile Red, was added in 3 mL of the aqueous polymer solution. The final concentration of the probe was, thus, fixed at  $1.7 \times 10^{-6}$  M. The maximum intensity of the emission peak of Nile Red in the region 600-650 nm, after excitation at 550 nm, was used to detect the formation of hydrophobic microdomains. The excitation and emission slits were fixed at 10 nm.

Dynamic Light Scattering and Electrophoresis Measurements.  $\zeta$ -potentials were determined by electrophoretic measurements, carried out at 25 °C by means of a NanoZetasizer, Nano ZS Malvern apparatus. The incident light source was a 4 mW He-Ne laser at 633 nm and the intensity of the scattered light was measured at 173°. The mean hydrodynamic diameter was determined from the obtained apparent diffusion coefficient through the Stokes-Einstein equation.

Transmission Electron Microscopy. TEM experiments were carried out using a JEM 2100 microscope operating at 200 kV. For the TEM investigation of pure NMPs,

diluted THF dispersions were used, whereas aqueous solutions/dispersions were used for the TEM investigation of pure polymers or MNPs/HMWSP hybrids. A drop of the solution/dispersion at the desired polymer concentration was deposited onto a carbon coated grid and allowed to evaporate at room temperature.

Zero-Field-Cooling/Field-Cooling (ZFC/FC). ZFC/FC measurements were performed at a Superconducting Quantum Interference Device (Quantum Design MPMS-5 SQUID); the sample was cooled from room temperature to 5 K without applying a magnetic field and then was heated back to room temperature under a magnetic field of 50 Oe, and blocking temperature value ( $T_b$ ) was obtained. Effective anisotropy constant ( $K_{\text{eff}}$ ) was calculated according to the equation:<sup>20</sup>  $25 \times k_B \times T_b = K_{\text{eff}} \times V$ , where  $k_B$  is the Boltzmann constant,  $T_b$  is the blocking temperature and  $V$  the particle volume.

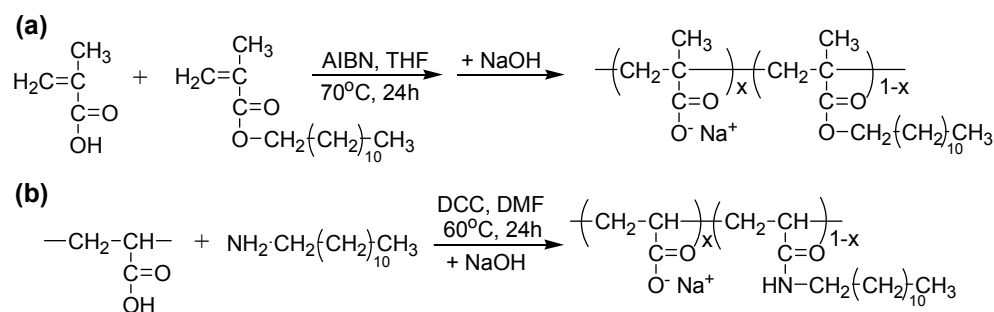
NMR Transverse Relaxation Time ( $T_2$ ).  $T_2$  measurements were performed at a 500-MR NMR Spectrometer (500 MHz, Agilent Technologies) at 25 °C, using a Carr-Purcell-Meiboom-Gill (CPMG) pulse sequence. The metal ion concentration (Fe +Co) of aqueous solutions was measured by inductively coupled plasma optical emission spectroscopy (ICP-OES).  $T_2$  was measured for a range of concentrations (0.05-0.8 mM) of metal ions of the aqueous suspensions of  $\text{CoFe}_2\text{O}_4@P(\text{ANa-co-DMAAm})$ ,  $\text{CoFe}_2\text{O}_4@CTAB$  and  $\text{CoFe}_2\text{O}_4@DMSA$ .

## Results and Discussion

### Synthesis and characterization of the copolymers

A series of HMWSP were evaluated in terms of their ability to stabilize hydrophobically modified  $\text{CoFe}_2\text{O}_4$  MNPs in water. These polymers, P(MANa-co-DMA), are based on a carboxylate backbone and dodecyl-side chains. As shown in

**Scheme 1a**, they have been prepared through free radical copolymerization (FRP) of MAA and DMA, followed by neutralization of the polyacid. Three P(MANa-co-DMA) copolymers differing in composition or molecular weight were successfully prepared by the variation of the monomers feed ratio and initiator/monomer ratio. Alternatively, a “grafting-to” methodology was applied to prepare an additional HMWSP, namely P(ANa-co-DAAm), through the coupling reaction of the carboxylic groups of PAA and the amine group of DAm using DCC as a condensing agent, also followed by neutralization of the product (**Scheme 1b**). A low molecular weight PAA homopolymer was used to synthesize the latter product.



**Scheme 1.** Synthesis of HMWSP: (a) P(MANa-co-DMA) and (b) P(ANa-co-DAAm) through FRP and “grafting-to” methodology, respectively.

The copolymers were characterized by <sup>1</sup>H-NMR and GPC as far as their chemical composition and molecular weight are concerned. For the characterization of the P(MANa-co-DMA), we took advantage of the solubility of the acid form of these polymers, P(MAA-co-DMA) in organic solvents. The <sup>1</sup>H-NMR spectra of the amphiphilic P(MAA-co-DMA) copolymers in d<sub>6</sub>-DMSO are shown in **Fig. 1**. The peaks in the region 1.3-2.2 ppm are attributed to the methyl- and methylene groups of the main polymer chain. The strong signal at ~1.3 ppm corresponds to the aliphatic groups of DMA while the signal at 0.8-0.9 ppm is attributed to the characteristic peak

of the  $-\text{CH}_3$  groups of both MAA and DMA. The same peaks are also observed in the  $^1\text{H-NMR}$  spectrum of P(ANa-co-DAAm) in  $\text{D}_2\text{O}$ , since its chemical structure is similar to that of P(MAA-co-DMA) copolymers. The major difference is that the peak at 0.8-0.9 ppm is now much sharper, as a consequence of the absence of the methyl group in the structure of sodium acrylate. The DMA content of the P(MAA-co-DMA) copolymers and the DAAm content of the P(ANa-co-DAAm) copolymer were determined from the integration ratio of the peaks at 0.8-0.9 ppm and 1.3 ppm. The results are shown in **Table 1**. As seen, P(MANa-co-DMA) copolymers with a hydrophobic content of  $\sim 25\%$  (mol/mol) and 12% (mol/mol) have been obtained. Moreover, the composition of the latter copolymer is close to that of the P(ANa-co-DMAAm) copolymer, derived through the “grafting-to” methodology.

GPC characterization of P(MAA-co-DMA) copolymers was performed in THF (**Fig. S1**). The number-average molecular weight ( $M_n$ ) and the weight-average molecular weight ( $M_w$ ) are tabulated in **Table 1**. As expected for FRP reactions, unimodal GPC curves with quite broad molecular weight distributions ( $M_w/M_n \sim 2-2.5$ ) are observed for all three copolymers. Moreover, through the adequate variation of the monomer/initiator molar ratio, copolymers with  $M_w$  ranging from  $\sim 14000$  up to 74000 g/mol are obtained. It was not possible to perform the GPC characterization of P(ANa-co-DAAm) in THF, due to its insolubility in organic solvents. Our attempts to perform the same characterization using an aqueous eluent were unsuccessful, probably due to the amphiphilic character of the copolymer in water. Nevertheless, we were able to calculate the molecular weight of the copolymer using the nominal mass of the precursor PAA and the chemical composition of the product, as determined through the  $^1\text{H-NMR}$  characterization. As seen in **Table 1**, this copolymer is

comparable with the P(MANa-co-DMA)3 sample, as it concerns both the hydrophobic content and the molecular weight.

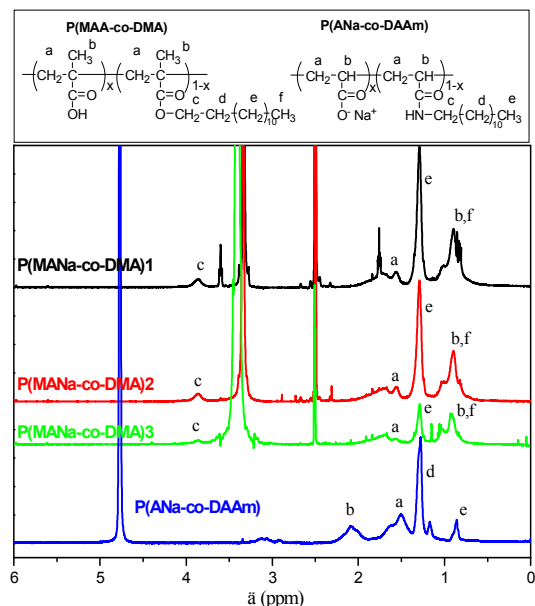


**Fig. 1**  $^1\text{H-NMR}$  spectra of the P(MAA-co-DMA) copolymers in  $\text{d}_6\text{-DMSO}$  and the copolymer P(ANa-co-DAAm) in  $\text{D}_2\text{O}$ .

**Table 1.** Physicochemical characterization results of the amphiphilic copolymers used in the present work.

Copolymer	Initiator/ monomer molar ratio	Composition ( $^1\text{H-NMR}$ ) <sup>a</sup>	$M_n$ , g/mol (GPC)	$M_w$ , g/mol (GPC)	$\zeta$ -potential, mV	CMC <sup>c</sup> , wt%
P(MANa-co-DMA)1	0.005	75	27800	73600	-40.7	0.002
P(MANa-co-DMA)2	0.015	77	10000	24600	-52.1	0.002
P(MANa-co-DMA)3	0.015	88	6400	13800	-49.7	0.2
P(ANa-co-DAAm)	-	90	-	7500 <sup>b</sup>	-46.8	0.1

<sup>a</sup> % moles of MANa or ANa units.

<sup>b</sup> Calculated from the nominal mass of PAA and the composition of the copolymer, as found through  $^1\text{H-NMR}$ .

<sup>c</sup> From Nile Red probing.

### Synthesis and characterization of the oleylamine coated $\text{CoFe}_2\text{O}_4$ nanoparticles

Bragg reflections in the  $2\theta$  range of  $10\text{-}90^\circ$  certify the formation of cobalt ferrite (PDF card no.22-1086). The characteristic peaks of the cubic spinel structure  $Fd3m$  (227) are evident in **Fig. 2a**; lattice parameter was calculated,  $8.401(0)$  Å and found close to the bulk value ( $a=8.392(1)$  Å) indicating the high crystallinity of the particles. The average crystalline size  $9.4(1)$  nm was estimated by Debye-Scherrer equation. Saturation magnetization ( $M_s$ ) of the MNPs was measured on a VSM (**Fig. 2b**). The normalized  $M_s$  was  $85$  emu/g which is close to the bulk<sup>21</sup> and the coercive field was  $283$  Oe. This value is among the highest for small sized  $\text{CoFe}_2\text{O}_4$  MNPs when compared to results reported in literature as for  $12$  nm  $M_s = 50.00$  emu/g (value corrected by TGA data),<sup>17</sup> for  $10$  nm  $M_s = 60.59$  emu/g (net magnetization value)<sup>22</sup> and for  $8$  nm  $M_s = 65.30$  emu/g (net magnetization value).<sup>23</sup> The magnetization enhancement can be attributed to oxygen vacancies in the spinel that reduce the dead layer (spin disorder layer structure)<sup>24</sup> meanwhile, reduction of the dead layer may be achieved through the coordination of  $\sigma$ -donors such as oleylamine, on the metal core since they can increase the spin-orbit coupling due to a decrease of the crystal field splitting which favors the uplift of the magnetocrystalline anisotropy of the surface layer.<sup>25</sup> **Fig. 2c** shows TEM image of oleylamine-coated  $\text{CoFe}_2\text{O}_4@OAm$  MNPs dispersed in THF. The nanoparticles are almost spherical with a relatively uniform size of  $9.0 \pm 0.15$  nm ( $\sigma = 1.5\%$ ) and narrow size distribution. In addition ZFC/FC measurements showed that the sample is in a ferrimagnetic state below  $T_b$  ( $T_b = 300$  K) (**Fig. S2**);  $K_{\text{eff}}$  was calculated  $29.7$  kJ/m<sup>3</sup>. Consequently, the resulted MNPs exhibit enhanced  $M_s$ , high anisotropy constant, relatively small size, high crystallinity and narrow size distribution characteristics that are essential for further applications.<sup>26</sup>

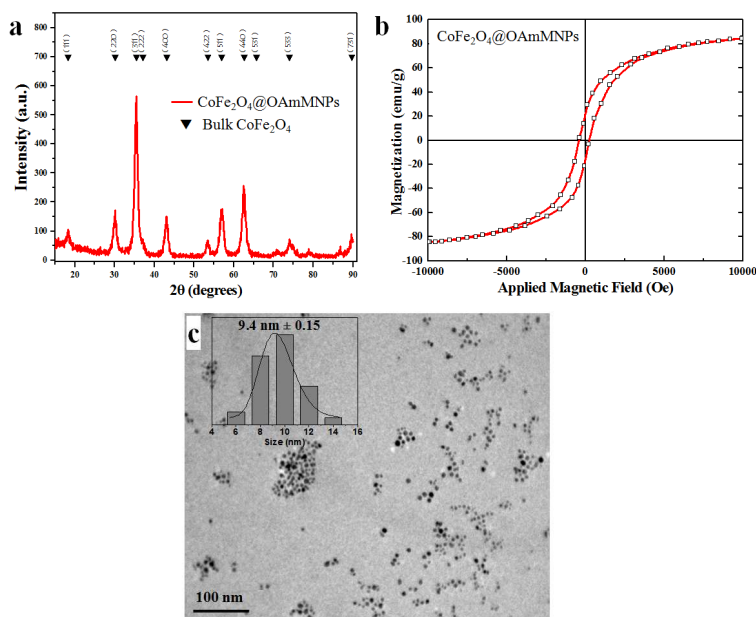


**Fig. 2** (a) X-Ray diffraction pattern of the as-prepared  $\text{CoFe}_2\text{O}_4@\text{OAm}$  MNPs, (b) VSM measurements and (c) TEM micrographs of  $\text{CoFe}_2\text{O}_4@\text{OAm}$  MNPs (scale bar: 100 nm).

### Use of HMWSP to transfer the hydrophobic $\text{CoFe}_2\text{O}_4@\text{OAm}$ MNPs in water

Self assembly of the amphiphilic copolymers in aqueous media. Before investigating the possibility of transferring the hydrophobic  $\text{CoFe}_2\text{O}_4@\text{OAm}$  MNPs in water with the help of the HMWSP used in the present study, the knowledge of the potential self-organization (eventually, forming micelle-like supramolecular structures) of the polymers in water is a prerequisite. Thus, we first determined the critical micelle concentrations (CMC) of the copolymers in aqueous solution through fluorescence probing using Nile Red as fluorescence probe. It is well known, that this probe is poorly soluble in water but its solubility increases in a less polar environment. Moreover, the probe is almost non-fluorescent in water and other polar solvents, whereas it is strongly fluorescent in less polar environments, showing an intense emission peak in the region 600-650 nm.



The maximum fluorescence intensity of the emission peak of Nile Red at 600-650 nm is plotted in **Fig. 3a** as a function of the concentration of the polymer. As it can be seen, for low polymer concentrations, the maximum intensity of Nile Red is low, indicating that the probe detects a purely hydrophilic environment. However when the polymer concentration increases above a critical value (CMC), the intensity increases sharply. Obviously, the amphiphilic copolymers are now self-organized in micellar-like structures, where the pendant alkyl chains form the hydrophobic core and the anionic polyelectrolyte backbones form the hydrophilic corona, stabilizing thus the system in water. As a consequence, the probe is now solubilized into the hydrophobic region of the formed polymeric micellar structures and “senses” a hydrophobic microenvironment. The CMC values of the amphiphilic copolymers are tabulated in **Table 1**. These values are low, since the hydrophobic content of the copolymers is rather high. Moreover, it is evident that CMC decreases drastically from ~0.1% (wt/v) to ~0.002% (wt/v) as the hydrophobic content of the copolymers increases from ~12% (mol/mol) to ~25% (mol/mol). Finally, it is clear that the crucial factor controlling CMC is the hydrophobic content and not the molecular weight (compare P(MANa-co-DMA)1 and P(MANa-co-DMA)2) or the exact chemical structure of the copolymer (compare P(MANa-co-DMA)3 and P(ANa-co-DAAm)). Moreover, since CMC depends on the chemical structure of the HMWSPs, the polymer concentration level is expected to be critical for the encapsulation (and consequently amount of MNPs, magnetization, etc) of CoFe<sub>2</sub>O<sub>4</sub>@OAm MNPs. For example, at a concentration C=0.005%wt, the copolymers P(MANa-co-DMA)3 and P(ANa-co-DAAm) are not expected to exhibit any encapsulation ability (C<CMC), while the copolymers P(MANa-co-DMA)1 and P(MANa-co-DMA)2 are expected to encapsulate the hydrophobic MNPs (C>CMC).

The size distribution and the charge of these supramolecular assemblies at concentrations above CMC were characterized through DLS and  $\zeta$ -potential measurements, respectively. As seen, in **Table 1**, strongly negative  $\zeta$ -potential values are measured for all copolymers, as a consequence of the anionic nature of the polyelectrolytes used. Such values are typical of micelles of amphiphilic diblock copolymers, consisted of a hydrophobic and an anionic PMANa block.<sup>27</sup>

The size distribution of the copolymers above CMC is shown in **Fig. 3b**. It is evident that several relaxation modes are present. In this representation of the DLS results, the slowest relaxation mode is identified by large sizes of the order of a few hundred nanometers. This slow mode is often observed in polyelectrolyte solutions at low ionic strength and it could be attributed to diffusive relaxation of cooperative multichain fluctuations or domains.<sup>28</sup> However, in the case of amphiphilic diblock copolymers could also correspond to large size objects, like large compound micelles.<sup>29</sup> Moreover, for all copolymers, an intermediate relaxation mode is also present, identified either as a shoulder or a clear population with a mean size of the order of a few tenths nanometers, corresponding to the polymeric micelles. Finally, in most cases, a fast relaxation mode is also present, corresponding to an average diameter of ~10-20 nm. This mode probably is that of single copolymer chains or unimolecular micelles.

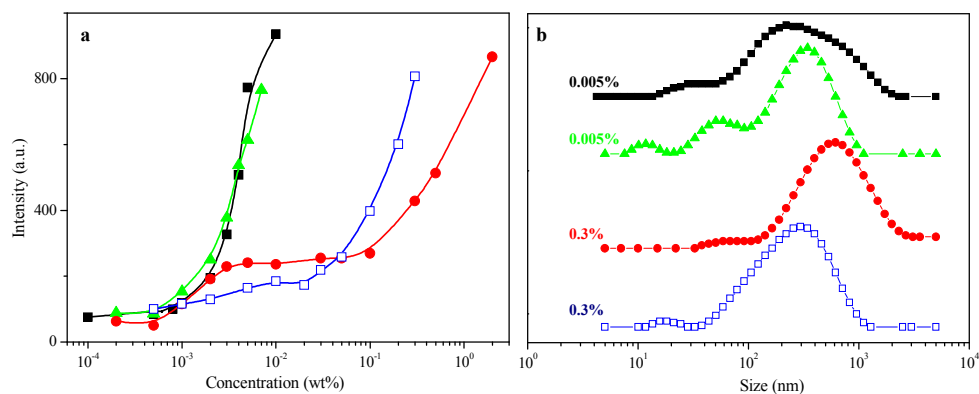


**Fig. 3** (a) Dependence of the maximum fluorescence intensity of the emission of Nile Red at 600-650 nm on the polymer concentration and (b) distribution of the hydrodynamic diameter, as determined by DLS for (■) P(MANa-co-DMA)1, (▲) P(MANa-co-DMA)2, (●) P(MANa-co-DMA)3 and (□) P(ANa-co-DAAm). The polymer concentrations for the DLS study, shown in the figure, are above CMC.

In order to gain more inside information on the supramolecular structures formed by the copolymers in aqueous solution, we proceeded to TEM characterization at concentrations below and above CMC. Some representative results concerning P(MANa-co-DMA)1 are shown in **Fig. 4**. Below the CMC the copolymer is molecularly dissolved in water and thus no special structures could be detected (**Fig. 4a**). Above CMC, the copolymer forms spherical structures, either micelles with a size of the order of ~30-40 nm (**Fig. 4b**) or large compound micelles with sizes corresponding to the slow relaxation mode observed through DLS (**insets of Fig. 4b**). A rather similar behavior was also observed for P(MANa-co-DMA)2. On the other hand, no isolated structures could be observed for P(MANa-co-DMA)3 and P(ANa-co-DAAm). This, apparently, is a consequence of the higher concentration used for the study, since the CMC values of the latter copolymers is much higher. Finally, it should be noted that both TEM and DLS techniques showed that the supramolecular structures formed are quite polydisperse in size. This polydispersity is probably a

consequence of the broad molecular weight distribution and the random architecture of our HMWSP.

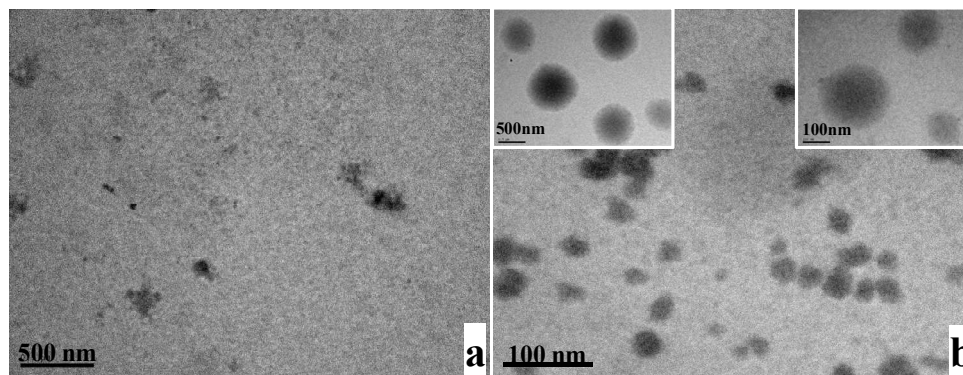


**Fig. 4** TEM images of (a) 0.001 wt% (below CMC, scale bar: 500 nm) and (b) 0.005 wt% (above CMC, scale bar: 100 nm) aqueous P(MANa-co-DMA)1 solutions. The scale bars in the insets are 500 nm (left) and 100 nm (right).

*Study of the  $\text{CoFe}_2\text{O}_4@HMWSP$  nanohybrids.* To transfer the hydrophobic  $\text{CoFe}_2\text{O}_4@OAm$  MNPs in water with the help of the aforementioned HMWSP, a solvent mixing protocol was applied. THF was chosen as organic solvent, because it is miscible with water and at the same time it is a good dispersant of the MNPs. In fact, when we applied this protocol using our HMWSP at a concentration below CMC, the hydrophobic  $\text{CoFe}_2\text{O}_4@OAm$  MNPs could not be dispersed in water and macroscopic phase separation was observed. On the other hand, as exemplified in **Scheme 2**, above CMC, the major part of the hydrophobic  $\text{CoFe}_2\text{O}_4@OAm$  MNPs (in the mixing ratio used) was able to enter in the hydrophobic cores of the micellar polymeric structures and MNPs were effectively stabilized in water. This was evidenced by the stable brownish coloration of the aqueous mixture (a representative photo at a high  $\text{CoFe}_2\text{O}_4@HMWSP$  concentration, corresponding to that of the NMR relaxivity measurements, is shown in **Scheme 2**).

Representative TEM images of the hydrophobic  $\text{CoFe}_2\text{O}_4@\text{P}(\text{MANa-co-DMA})_1$  mixtures below and above CMC, using this protocol, are shown in **Fig. 5a** and **5b**, respectively. Below CMC, no micelles are formed and no MNPs could be detected on the TEM grid. In agreement with the discussion in Fig. 3a, when the copolymer is molecularly dissolved in water, the polymeric chains are not capable of dispersing the hydrophobic magnetic nanoparticles in aqueous solution (**Fig. 5a**). On the other hand, at a polymer concentration higher than CMC, one can observe the effective encapsulation of the magnetic nanoparticles in the formed polymer micelle-like structures (**Fig. 5b**). The hydrophobic  $\text{CoFe}_2\text{O}_4@\text{OAm}$  MNPs are located in the hydrophobic core of the micelles formed by  $\text{P}(\text{MANa-co-DMA})_1$ , while the hydrophilic MANa groups maintain the whole system stable in water. A similar behavior is also exhibited by the hydrophobic  $\text{CoFe}_2\text{O}_4@\text{P}(\text{MANa-co-DMA})_2$ , as well (**Fig. 5c**). In the TEM images, as a consequence of the high contrast of the MNPs, the hydrophilic part of the micelles cannot be seen but only the hydrophobic cores with the incorporated  $\text{CoFe}_2\text{O}_4@\text{OAm}$  MNPs are observable. In fact, for this reason, we were also able to observe the nanohybrid structures formed upon mixing the hydrophobic  $\text{CoFe}_2\text{O}_4@\text{OAm}$  MNPs with  $\text{P}(\text{MANa-co-DMA})_3$  (**Fig. 5d**) and  $\text{P}(\text{ANa-co-DAAm})$  (**Fig. 5e**), although a rather high polymer concentration is used in order to ensure the micellization of the copolymers. It is noteworthy that the size distribution of the cores of the  $\text{CoFe}_2\text{O}_4@\text{HMWSP}$  nanohybrids is large. Thus, in a rather good qualitative agreement with the DLS findings of **Fig. 3b**,  $\text{CoFe}_2\text{O}_4$ -loaded cores of a large size (more than 100 nm), corresponding to large-compound micelles, as well as of smaller sizes (few tenths of nanometers), corresponding to polymeric micelles, are observable for most nanohybrids. In fact, it is interesting to note that assemblies of nanohybrids corresponding to polymeric micelles are mainly observed

in the case of P(MANa-co-DMA)2 copolymer. This is in line with the DLS findings, where the population of polymeric micelles is more pronounced, as compared to the other copolymers.

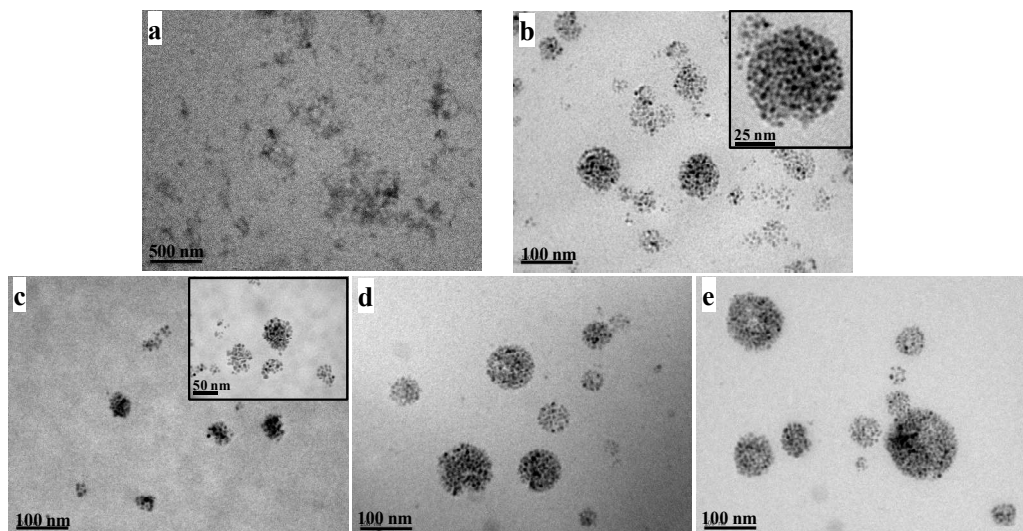
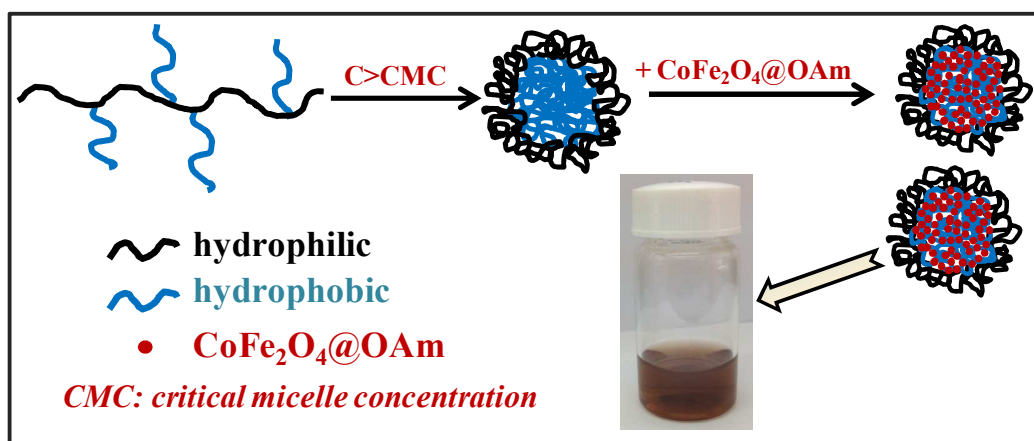


**Fig. 5** TEM images of  $\text{CoFe}_2\text{O}_4@\text{P}(\text{MANa-co-DMA})_1$  (a) below CMC (0.001 wt%), scale bar: 500 nm) and (b) above CMC (0.005 wt%); (c)  $\text{CoFe}_2\text{O}_4@\text{P}(\text{MANa-co-DMA})_2$  above CMC (0.005 wt%), (d)  $\text{CoFe}_2\text{O}_4@\text{P}(\text{MANa-co-DMA})_3$  above CMC (0.3 wt%) and (e)  $\text{CoFe}_2\text{O}_4@\text{P}(\text{ANa-co-DAAm})$  above CMC (0.3 wt%). The scale bars of b-e are 100 nm, while the scale bars of insets in b and c are 25 nm and 50 nm, respectively.



**Scheme 2.** Schematic depiction of the stabilization of  $\text{CoFe}_2\text{O}_4@\text{HMWSP}$  nanohybrids in water.

### NMR Relaxation Measurements

The characteristics of the as-prepared  $\text{CoFe}_2\text{O}_4@\text{OAm}$  MNPs ( $D=9.4$  nm,  $M_s=85$  emu/gr,  $K_{\text{eff}}=29.7$  kJ/m<sup>3</sup>) rendered them challenging candidates for potential bioapplications including Magnetic Resonance Imaging (MRI) as they exhibited enhanced  $M_s$ , small size, narrow size distribution and  $K_{\text{eff}}$  values that are among the proposed optimum values which are  $10 < D < 30$  nm,  $60 < M_s < 100$  emu/g and  $5 < K_{\text{eff}} < 40$  KJ/m<sup>3</sup>.<sup>30</sup> The efficiency of the MNPs to act as  $T_2$  contrast agents for MRI depends on the relaxation process of protons when placed in an external magnetic field, namely the transverse or spin-spin relaxation process ( $T_2$ ) while they have a much smaller effect on the longitudinal or spin-lattice relaxation process ( $T_1$ ). The transverse  $T_2$  relaxation time of hydrogen protons of pure water at various concentrations of the samples were determined using an NMR spectrometer. Moreover, the efficiency of the MNPs to act as  $T_2$  contrast agents is determined in terms of the transverse relaxivity ( $r_2$ ) according to equation (1).<sup>31</sup> For comparison reasons, three different methodologies were applied to convert the as-prepared hydrophobic  $\text{CoFe}_2\text{O}_4@\text{OAm}$  MNPs to hydrophilic and the transverse relaxivity ( $r_2$ ) of each system at various concentrations have been determined: i) addition of a coating layer (CTAB), ii) ligand exchange procedure (DMSA) and iii) polymer encapsulation (P(ANa-co-DAAm)).

$$R_2 = \frac{1}{T_2} = \frac{1}{T_2^0} + r_2 \cdot C \quad (1)$$

where  $T_2$  is the observed proton relaxation time in the presence of MNPs,  $T_2^0$  is the proton relaxation time of pure water and  $C$  is the concentration of the contrast agent.  $T_2$  was measured for a range of concentrations (0.05-0.8 mM) of metal ions of the aqueous suspensions of  $\text{CoFe}_2\text{O}_4@\text{P(ANa-co-DMAAm)}$ ,  $\text{CoFe}_2\text{O}_4@\text{CTAB}$  and  $\text{CoFe}_2\text{O}_4@\text{DMSA}$ . All measurements showed perfect monoexponential decay, which is characteristic for magnetic compounds that enhance the water proton relaxivity by

diffusion. Indeed, a linear concentration dependence of  $r_2$  is experimentally observed (**Fig. 6**), permitting the determination of  $r_2$  for the resulted hydrophilic MNPs obtained through the three surface modification procedures. In addition, the  $\zeta$ -potential of these hydrophilic MNPs was determined as an indicator of the good colloidal stability of the aqueous suspensions.<sup>32</sup>  $\zeta$ -potential and  $r_2$  values are summarized in **Table 2**.  $\text{CoFe}_2\text{O}_4@\text{P(ANa-co-DAAm)}$  was selected among the  $\text{CoFe}_2\text{O}_4@\text{HMWSP}$  nanohybrids since it bears a comparable surface charge (absolute value) with  $\text{CoFe}_2\text{O}_4@\text{CTAB}$ . The negative charge of  $\text{CoFe}_2\text{O}_4@\text{DMSA}$  and  $\text{CoFe}_2\text{O}_4@\text{P(ANa-co-DAAm)}$  MNPs is attributed to the  $-\text{COO}^-$  groups, while the positive charge of  $\text{CoFe}_2\text{O}_4@\text{CTAB}$  MNPs is due to the  $-\text{N}^+(\text{CH}_3)_3$  functional group.

The  $r_2$  relaxivity value of  $\text{CoFe}_2\text{O}_4@\text{P(ANa-co-DAAm)}$  is lower to that of  $\text{CoFe}_2\text{O}_4@\text{CTAB}$  while it is  $\sim 4$  times higher than that of  $\text{CoFe}_2\text{O}_4@\text{DMSA}$ . This difference is attributed to the structure and size of each coating agent. The metal core of  $\text{CoFe}_2\text{O}_4@\text{P(ANa-co-DAAm)}$  is effectively isolated from the exterior water molecules since it is confined within the hydrophobic polymer core (**Fig. 5e**).<sup>33</sup> The dramatic decrease of the  $r_2$  value in the case of  $\text{CoFe}_2\text{O}_4@\text{DMSA}$  is associated with the lower colloidal stability and the formation of a shell-like extended coating. DMSA would be expected to increase  $r_2$  values, since it is a small ligand with carboxylic groups. However, an opposite effect on  $r_2$  relaxivity is observed. The anchored carboxyl groups ( $\text{COO}^-$ ) formed a shell-like stable coating, later on reinforced by the disulfide (S-S) cross-linking between different DMSA molecules.<sup>34</sup> The presence of free carboxylic groups as well as the absence of  $-\text{SH}$  groups has been certified by the FT-IR spectra (**Fig. S3**). An analogous behavior was observed previously by us for  $\text{NiFe}_2\text{O}_4$  nanoparticles modified with CTAB and DMSA.<sup>35</sup>



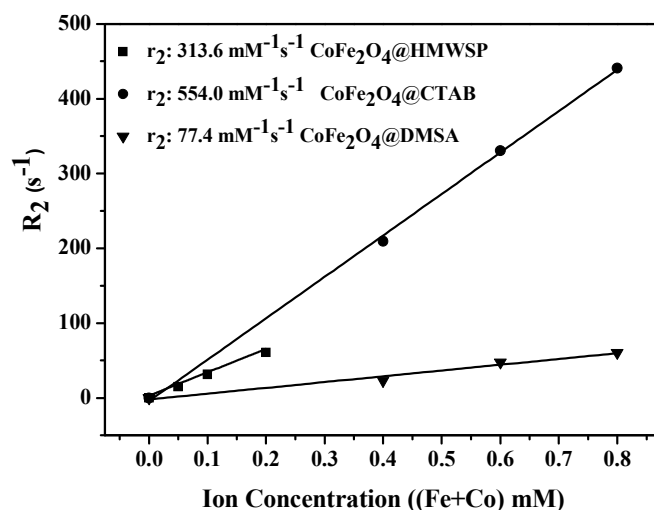


**Fig. 6** Transverse relaxation measurements of aqueous suspensions of CoFe<sub>2</sub>O<sub>4</sub>@P(ANa-co-DAAm) (■), CoFe<sub>2</sub>O<sub>4</sub>@CTAB (●) and CoFe<sub>2</sub>O<sub>4</sub>@DMSA (▼).

However, CoFe<sub>2</sub>O<sub>4</sub>@CTAB and CoFe<sub>2</sub>O<sub>4</sub>@P(ANa-co-DAAm) formed better aqueous colloidal dispersions than CoFe<sub>2</sub>O<sub>4</sub>@DMSA. Nevertheless, all samples affected relaxivity in a positive way and afforded  $r_2$  values comparable and even higher than those previously reported for CoFe<sub>2</sub>O<sub>4</sub> MNPs at similar sizes. For instance CoFe<sub>2</sub>O<sub>4</sub> MNPs of 8 nm following a similar ligand exchange procedure where oleic acid and oleylamine are exchanged with DMSA, the  $r_2$  value was found 392.4 mM<sup>-1</sup>s<sup>-1</sup> ( $T_2$  values recorded at 9.4 T),<sup>23</sup> while for spherical CoFe<sub>2</sub>O<sub>4</sub> MNPs with sizes 6 nm, 10 nm and 15 nm following a phase transfer procedure with the capping agent 11-amino undecanoic acid ( $T_2$  values recorded at 3 T) found to be equal to 110.9 mM<sup>-1</sup>s<sup>-1</sup>, 169.9 mM<sup>-1</sup>s<sup>-1</sup> and 301.8 mM<sup>-1</sup>s<sup>-1</sup>, respectively.<sup>22</sup> Also, Yang et al.<sup>31</sup> by employing additional amphiphilic surfactants (anionic, cationic and neutral) through hydrophobic interactions around CoO MNPs, observed different  $r_2$  values which is associated with the different structure of the coatings ( $T_2$  values recorded at 0.5 T). Moreover, the presented values herein are much higher compared to  $\gamma$ -Fe<sub>2</sub>O<sub>3</sub> MNPs as  $r_2$  values

increased from 13 to 64  $\text{mM}^{-1}\text{s}^{-1}$ , with respect to the decreasing thickness of silica layer<sup>36</sup> in a 500 MHz NMR spectrometer.

**Table 2.**  $\zeta$ -potential and  $r_2$  relaxivity values of  $\text{CoFe}_2\text{O}_4$  MNPs with different coatings in water.

Sample	Surface Coating	$\zeta$ -potential (mV)	$r_2$ ( $\text{mM}^{-1}\text{s}^{-1}$ )
$\text{CoFe}_2\text{O}_4@\text{CTAB}$	CTAB	+34.4	554.0
$\text{CoFe}_2\text{O}_4@\text{P(ANa-co-DAAm)}$	P(ANa-co-DAAm)	-38.0	313.8
$\text{CoFe}_2\text{O}_4@\text{DMSA}$	DMSA	-19.8	77.4

## Conclusions

The use of MNPs for new biomedical applications requires aqueous dispersion and further functionalization. Thus, tailoring the surface and understanding the surface characteristics are necessary. In the present work, we took advantage of hydrophobically modified water-soluble polymers, HMWSP, to achieve these prerequisites in the case of hydrophobic MNPs. These HMWSP, comprised by a poly(sodium methacrylate) or poly(sodium acrylate) backbone and pendent dodecyl methacrylate or dodecyl acrylamide chains, respectively, were synthesized through copolymerization or “grafting-to” methodologies. As a consequence of their amphiphilic character, these copolymers self organize in aqueous media, forming supramolecular micellar structures above the critical micellization concentration (CMC), while they are molecularly dissolved in water below CMC. The micellar structures are characterized by a high polydispersity in size due to the broad molecular weight distribution and the random architecture of the HMWSP. In fact, for most polymers, single polymer chains, simple micelles and large-compound micelles were detected through DLS, while the last two populations were also

visualized through TEM. Moreover, it is shown that the crucial factor controlling CMC is the hydrophobic content and not the molar mass of the copolymers.

The hydrophobic  $\text{CoFe}_2\text{O}_4@OAm$  MNPs (9.4 nm) were successfully encapsulated into the hydrophobic cores of the micellar structures of the copolymers above CMC, forming  $\text{CoFe}_2\text{O}_4@HMWSP$  nanohybrids which are well stabilized in water by the hydrophilic backbones of the HMWSP. To the best of our knowledge such studies are scarcely reported in literature. Moreover, a representative example of  $\text{CoFe}_2\text{O}_4@HMWSP$  nanohybrids,  $\text{CoFe}_2\text{O}_4@P(ANa-co-DAAm)$ , exhibited a sufficiently large  $r_2$  value ( $313.6 \text{ mM}^{-1}\cdot\text{s}^{-1}$ ), rendering the HMWSP-mediated stabilization of hydrophobic MNPs an attractive technique for the preparation of potential  $T_2$ -contrast agents. Finally, the chemical composition of the synthesized amphiphilic polymers can be tailored, allowing fine-tuning of the properties of the  $\text{MNPs}@HMWSP$  nanohybrids that would lead to multi-responsive/multi-sensing water-dispersible  $\text{MNPs}@HMWSP$  nanohybrids.

### Acknowledgements

This research has been co-financed by the European Union (European Social Fund–ESF) and Greek national funds through the Operational Program "Education and Lifelong Learning" of the National Strategic Reference Framework (NSRF)-Research Funding Program: THALES. Investing in knowledge society through the European Social Fund. The authors thank Dr Maria Kollia from the Lab of Electron Microscopy and Microanalysis at the University of Patras for the TEM images.

## References

- 1 (a) S. E. Webber, *J. Phys. Chem. B*, 1998, **102**, 2618-2626; (b) K. Kataoka, A. Harada and Y. Nagasaki, *Adv. Drug Deliv. Rev.*, 2001, **47**, 113-131; (c) G. Riess, *Prog. Polym. Sci.*, 2003, **28**, 1107-1170; (d) J.-F. Gohy, *Adv. Polym. Sci.*, 2005, **190**, 65-136; (e) A. Blanz, S. P. Armes and A. J. Ryan, *Macromol. Rapid Commun.*, 2009, **30**, 267-270.
- 2 (a) N. Hadjichristidis, M. Pitsikalis and H. Iatrou, *Adv. Polym. Sci.*, 2005, **189**, 1-124; (b) H. Cui, Z. Chen, S. Zhong, K. L. Wooley and D. J. Pochan, *Science*, 2007, **317**, 647-650; (c) A. E. Smith, X. Xu and C. L. McCormick, *Prog. Polym. Sci.*, 2010, **35**, 45-93; (d) Y. Mai and A. Eisenberg, *Chem. Soc. Rev.*, 2012, **41**, 5969-5985; (e) A. M. Budgin, Y. A. Kabachii, Z. B. Shifrina, P. M. Valetsky, S. S. Kochev, B. D. Stein, A. Malyutin, L. M. Bronstein, *Langmuir*, 2012, **28**, 4142-4151.
- 3 (a) C. Q. Wang, G. T. Li and R. R. Guo, *Chem. Commun.*, 2005, 3591-3593; (b) R. C. W. Liu, A. Pallier, M. Brestaz, N. Pantoustier and C. Tribet, *Macromolecules*, 2007, **40**, 4276-4286; (c) T. Kawata, A. Hashizume and T. Sato, *Macromolecules*, 2007, **40**, 1174-1180; (d) Y. Li, Y. Zhang, D. Yang, C. Feng, S. Zhai, J. Hu, G. Lu and X. Huang, *J. Polym. Sci. Part A: Polym. Chem.*, 2009, **47**, 6032-6043; (e) Y. Ogata, M. Iwano, T. Mogi and Y. Makita, *J. Polym. Sci. Part B: Polym. Phys.*, 2011, **49**, 1651-1659.
- 4 (a) K. T. Wang, I. Iliopoulos and R. Audebert, *Polym. Bull.*, 1988, **20**, 577-582; (b) J. E. Klijn, J. Kevelam and J. B. F. N. Engberts, *J. Colloid Interface Sci.*, 2000, **226**, 76-82.
- 5 (a) F. Candau and J. Selb, *Adv. Colloid Interface Sci.*, 1999, **79**, 149-172; (b) L. Guillaumont, G. Bokias, I. Iliopoulos, *Macromol. Chem. Phys.*, 2000, **201**, 251-260; (c) K. Podhajecka, K. Prochazka and D. Hourdet, *Polymer*, 2007, **48**, 1586-1595.
- 6 (a) M. F. Francis, M. Piredda and F. M. Winnik, *J. Control. Release*, 2003, **93**, 59-68; (b) E. Rotureau, E. Marie, E. Dellacherie and A. Durand, *Colloid Surface A*, 2007, **301**, 229-238; (c) E. V. Korchagina and O. E. Philippova, *Langmuir*, 2012, **28**, 7880-7888; (d) R. Covis, C. Ladaviere, J. Desbrieres, E. Marie and A. Durand, *Carbohydr. Polym.*, 2013, **95**, 360-365.
- 7 J. Kötz, S. Kosmella and T. Beitz, *Prog. Polym. Sci.*, 2001, **26**, 1199-1232.

- 8 (a) O. E. Philippova and A. R. Khokhlov, *Petrol. Chem.*, 2010, **50**, 266-270; (b) D. A. Z. Wever, F. Picchioni and A. A. Broekhuis, *Prog. Polym. Sci.*, 2011, **36**, 1558-1628.
- 9 (a) T. Osaka, T. Matsunaga, T. Nakanishi, A. Arakaki, D. Niwa, and H. Iida, *Anal. Bioanal. Chem.*, 2006, **384**, 593-600; (b) J. L. Corchero and A. Villaverde, *Trends Biotechnol.*, 2009, **27**, 468-476; (c) S. A. Corr, Y. P. Rakovich and Y. K. Gun'ko, *Nanoscale Res. Lett.*, 2008, **3**, 87-104.
- 10 (a) Y. Wang, C. Xu and H. Ow, *Theranostics*, 2013, **3**, 544-560; (b) H. M. Joshi, *J. Nanopart. Res.*, 2013, **15**, 1235.
- 11 (a) X. Jia, D. Chen, X. Jiao, T. He, H. Wang, W. Jiang, *J. Phys. Chem. C*, 2009, **112**, 911-917; (b) D. Peddis, F. Orrù, A. Ardu, C. Cannas, A. Musinu and G. Piccaluga, *Chem. Mater.*, 2012, **24**, 1062-1071.
- 12 R. A. Sperling and W. J. Parak, *Phil. Trans. R. Soc. A*, 2010, **368**, 1333-1383.
- 13 (a) H. Ai, C. Flask, B. Weinberg, X. Shuai, M. D. Pagel, D. Farrell, J. Duerk and J. Gao, *Adv. Mater.*, 2005, **17**, 1949-1952; (b) B.-Su. Kim, J.-M. Qiu, J.-P. Wang and T. A. Taton, *Nano Lett.*, 2005, **5**, 1987-1991; (c) S. Lecommandoux, O. Sandre, F. Checot, J. Rodriguez-Hernandez and R. Perzynski, *Adv. Mater.*, 2005, **17**, 712-718; (d) S. Lecommandoux, O. Sandre, F. Checot and R. Perzynski, *Prog. Solid State Chem.*, 2006, **34**, 171-179; (e) J. Yang, E.-K. Lim, H. J. Lee, J. Park, S. C. Lee, K. Lee, H.-G. Yoon, J.-S. Suh, Y.-M. Huh and S. Haam, *Biomaterials*, 2008, **29**, 2548-2555; (f) A. Bakandritsos, G. Mattheolabakis, R. Zboril, N. Bouropoulos, J. Tucek, D. G. Fatouros and K. Avgoustakis, *Nanoscale*, 2010, **2**, 564-572; (g) S. Mahajan, V. Koul, V. Choudhary, G. Shishodia and A. C. Bharti, *Nanotechnology*, 2013, **24**, 015603; (h) D.-H. Kim, E. A. Vitol, J. Liu, S. Balasubramanian, D. J. Gosztola, E. E. Cohen, V. Novosad and E. A. Rozhkova, *Langmuir*, 2013, **29**, 7425-7432.
- 14 (a) E. V. Shtykova, X. Huang, X. Gao, J. C. Dyke, A. L. Schmucker, B. Dragnea, N. Remmes, D. V. Baxter, B. Stein, P. V. Konarev, D. I. Svergun and L. M. Bronstein, *J. Phys. Chem. C*, 2008, **112**, 16809-16817; (b) L. M. Bronstein, E. V. Shtykova, A. Malyutin, J. C. Dyke, E. Gunn, X. Gao, B. Stein, P. V. Konarev, B. Dragnea and D. I. Svergun, *J. Phys. Chem. C.*, 2010, **114**, 21900-21907; (c) X. Li, H. Li, G. Liu, Z. Deng, S. Wu, P. Li, Z. Xu, H. Xu and P. K. Chu, *Biomaterials*, 2012,

- 33, 3013-3024; (d) E. Peng, E. S. G. Choo, Y. Sheng and J. M. Xue, *New J. Chem.*, 2013, **37**, 2051-2060.
- 15 V. Georgiadou, C. Kokotidou, B. Le Droumaguet, B. Carbonnier, T. Choli-Papadopoulou and C. Dendrinou-Samara, *Dalton Trans.* DOI:10.1039/C3DT53179A.
- 16 Y. Tian, B. Yu, X. Li and K. Li, *J. Mater. Chem.*, 2011, **21**, 2476-2481.
- 17 L. I. Cabrera, A. Somoza, J. F. Marco, C. J. Serna and M. P. Morales, *J. Nanopart. Res.*, 2012, **14**, 873.
- 18 (a) A. G. Roca, S. Veintemillas-Verdaguer, M. Port, C. Robic, C. J. Serna and M. P. Morales, *J. Phys. Chem. B*, 2009, **113**, 7033-7039; (b) A. Ruiz, G. Salas, M. Calero, Y. Hernandez, A. Villanueva, F. Herranz, S. Veintemillas-Verdaguer, E. Martinez, D. F. Barber and M. P. Morales, *Acta Biomater.*, 2013, **9**, 6421-6430.
- 19 A. Patterson, *Phys. Rev.*, 1939, **56**, 978-982.
- 20 E. F. Kneller and F. E. Luborsky, *J. Appl. Phys.*, 1963, **34**, 656-658.
- 21 I. Sharifi, H. Shokrollahi, M. M. Doroodmand and R. Safi, *J. Magn. Magn. Mater.*, 2012, **324**, 1854-1861.
- 22 H. M. Joshi, Y. P. Lin, M. Aslam, P. V. Prasad, E. A. Schultz-Sikma, R. Edelman, T. Meade and V. P. Dravid, *J. Phys. Chem. C*, 2009, **113**, 17761-17767.
- 23 D.-H. Kima, H. Zeng, T. C. Ng and C. S. Brazel, *J. Magn. Magn. Mater.*, 2009, **321**, 3899-3904.
- 24 M. Y. Rafique, L. Pan, Q. Javed, M. Z. Iqbal and L. Yang, *J. Nanopart. Res.*, 2012, **14**, 1189.
- 25 J. Mohapatra, A. Mitra, D. Bahadur and M. Aslam, *CrystEngComm*, 2013, **15**, 524-532.
- 26 E. Solano, L. Perez-Mirabet, F. Martinez-Julian, R. Guzman, J. Arbiol, T. Puig, X. Obradors, R. Yanez, A. Pomar, S. Ricart and J. Ros, *J. Nanopart. Res.*, 2012, **14**, 1034.
- 27 M. Milnera, M. Stepanek, I. Zuskova, and K. Prochazka, *Int. J. Polym. Anal. Ch.*, 2007, **12**, 23-33.
- 28 B. D. Ermi and E. J. Amis, *Macromolecules*, 1998, **31**, 7378-7384.
- 29 J. Yao, P. Ravi, K. C. Tam and L. H. Gan, *Langmuir*, 2004, **20**, 2157-2163.

- 30 J.-H. Lee, J.-t. Jang, J.-s. Choi, S. H. Moon, S.-h. Noh, J.-w. Kim, J.-G. Kim, I.-S. Kim, K. I. Park and J. Cheon, *Nat. Nanotechnol.*, 2011, **6**, 418-422.
- 31 H. Yang, H. Zhou, C. Zhang, X. Li, H. Hu, H. Wu and S. Yang, *Dalton Trans.*, 2011, **40**, 3616-3621.
- 32 Y. Xu, Y. Qin, S. Palchoudhury and Y. Bao, *Langmuir*, 2011, **27**, 8990-8997.
- 33 S. Tong, S. Hou, Z. Zheng, J. Zhou and G. Bao, *Nano Lett.*, 2010, **10**, 4607-4613.
- 34 Z. P. Chen, Y. Zhang, S. Zhang, J. G. Xia, J. W. Liu, K. Xu and N. Gu, *Colloid Surface*, 2008, **316**, 210-216.
- 35 M. Menelaou, K. Georgoula, K. Simeonidis, C. Dendrinou-Samara, *Dalton Trans.*, 2014, **43**, 3626-3636.
- 36 S. L. C. Pinho, G. A. Pereira, P. Voisin, J. Kassem, V. Bouchaud, L. Etienne, J. A. Peters, L. Carlos, S. Mornet, C. F. G. C. Geraldes, J. Rocha and M-H. Delville, *ACS Nano*, 2010, **4**, 5339-5349.

## Table of contents

### Application of hydrophobically modified water-soluble polymers for the dispersion of hydrophobic magnetic nanoparticles in aqueous media

Z. Iatridi, V. Georgiadou, M. Menelaou, C. Dendrinou-Samara\* and G. Bokias\*

Oleylamine-coated  $\text{CoFe}_2\text{O}_4$  magnetic nanoparticles were successfully encapsulated into hydrophobically modified water-soluble polymers. The resulted hydrophilic nano hybrids exhibit promising  $r_2$ -relaxivity properties.

